# Fold-Speed Control in Collapsing Mixed Phospholipid Monolayers

## Yi Zhang and Thomas M. Fischer*

*Department of Chemistry and Biochemistry, Florida State University, Tallahassee, Florida 32306*

*Received: June 17, 2004; In Final Form: November 9, 2004*

Mixed monolayers of dipalmitoylphosphatidylcholine (DPPC) and dipalmitoyl-phosphatidylserine are compressed beyond their collapse pressure. Primary and secondary folds that grow perpendicular to the compression direction are observed using Brewster angle microscopy. The secondary fold velocity is measured with a fast charge-coupled device camera. We observe a reduction in secondary fold speed when increasing the mole fraction of the softer DPPC component in the monolayer. The fracture kinetics follows theoretical predictions for the fold coarsening dynamics of uniaxially stressed three-dimensional systems.

## Introduction

Monolayer collapse is a certain two-dimensional (2D) to three-dimensional (3D) transformation of a Langmuir monolayer occurring at air/water interfaces upon the overcompression of the densely packed, insoluble, amphiphilic film. The *collapse pressure,* $\pi_c$, at which collapse appears depends on the rate of compression and levels off at the *equilibrium spreading pressure*[1] $\pi_e$ if compressed adiabatically with an infinitely slow compression rate. A rich variety of collapse scenarios that differ in how the material is ejected from the monolayer into the subphase or on top of the monolayer has been observed using Brewster angle,[2] light scattering,[3−5] phase contrast,[6,7] fluorescence,[8] electron,[9] and atomic force microscopy.[5] These experiments prove that the collapsing behavior of monolayers is strongly governed by structural properties of the film, such as the order of the phase[2] or coexisting phases,[4,8] prior to collapse. Collapse can be reversible or irreversible such that the monolayer can or cannot be recovered upon expansion. Reversible collapse includes the nucleation of 3D buds[3] or vesicles,[8] the buckling of the monolayer with a bilayer being expelled and folded on top of the monolayer.[9] The monolayer may also fold into the subphase with small height differences between two coexisting phases serving as heterogeneous nucleation sites for the folds.[5,8] Roughening of the monolayer upon collapse has been observed by Schief[4] and by Hatta.[6,7] Reversible elliptical folds in collapsing monolayers could be explained by the self-attraction of the deformable opposing monolayer surfaces that fold into the subphase.[5] The mathematics describing these reversible folds is identical to that of Griffith Cracks[10] in solids with only the sign of the displacement and stress field being reversed.

The mathematical similarity between cracks in solids and folds in monolayers raises the question, can the collapse kinetics of monolayer collapse be treated similarly to what has been done for the crack growth dynamics in solids?[11−15] For example, Brener et al.[11] emphasized that the interaction between parallel cracks during the coarsening of cracks in a uniaxially strained solid leads to a constant crack velocity and a ripening of the cracks that behaves similar to Ostwald ripening in a first-order phase transition. The Einstein ice-skater model focused on the

bond-breaking event of the crack-tip atom; thus, the steady-state crack velocity can be predicted quantitatively.[12] More recently, the dynamic behavior of cracks going through nonideal brittle materials and propagating in far-from equilibrium processes has also been discussed.[13,14]

In a previous paper, we have observed three types of collapse patterns: surface roughening, random network, and anisotropic collapse, in different fatty acid monolayers upon compression. We also found that the rates of modulated growing ejected amphiphilic material are significantly influenced by slight changes in pH and concentration of $Co^{2+}$ ions. In the current work, we focus on how to influence the velocity of anisotropic irreversible folds by varying the composition of a binary mixed lipid monolayer. Here we show morphologies of irreversible folds propagating through binary L-$\alpha$-dipalmitoylphosphatidylcholine (DPPC)/1,2-dipalmitoyl-*sn*-glycero-3-[phosphor-L-serine] (sodium salt) (DPPS) mixtures, using a fast charge-coupled device (CCD) camera fixed to a Brewster angle microscope (BAM). We measure the fold propagation speeds to obtain information on the collapse behavior, texture, and dynamics.

## Experiment Section

**Materials.** DPPC and DPPS were purchased from Avanti Polar-lipid, Inc., and used without further purification (99+% purity). Chloroform with 99+% purity was from Fisher, Inc. Deionized ultrapure water, (MilliQ system, 18.3 MΩ) was used as aqueous subphase solution in order to avoid salt crystallization under the transferred film. All experiments were performed at room temperature (19−21 °C).

**Method.** A home-built BAM was mounted on a homemade single-barrier Langmuir trough, using a CCD camera (FastCam super 10 K with Kodak Motion corder analyzer Ps-220, Video Kommunikation GMBH) as the video recorder with frequency 250 frames/s. The laser beam (wavelength of 514 nm, Innova 90 C, Coherent) for the BAM was operated at a power of 500 mW to give sufficient intensity for the high speed recording. No scanning of the focus of the BAM image was performed (usually done to have the entire image in focus) since it interferes with the fast recording of the fold propagation.

A profilometer (KIA Tencor P15.) was used to measure transferred collapse patterns in the contact mode. Each sample was transferred to a hydrophilic-treated silicon wafer by the Langmuir−Schäfer technique. A silicon wafer had been im-

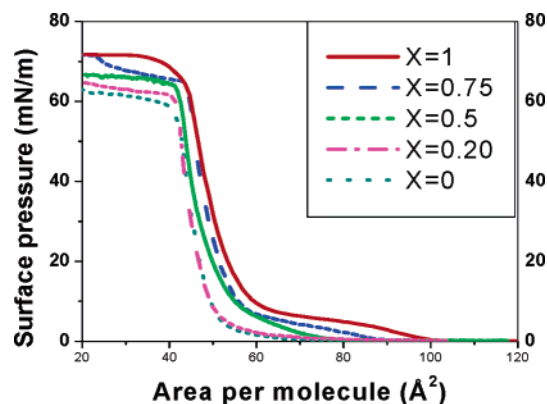* To whom correspondence may be addressed. E-mail: tfischer@chem.fsu.edu.

Fold Speed in Monolayers

*J. Phys. Chem. B, Vol. 109, No. 8, 2005* **3443**



**Figure 1.** Pressure vs area isotherms of mixed DPPC/DPPS monolayers for different mole fractions $x$ of DPPC. Collapse pressures of low $x$ monolayers are around 60 mN/m and rise to almost the surface tension of water for high values of $x$.
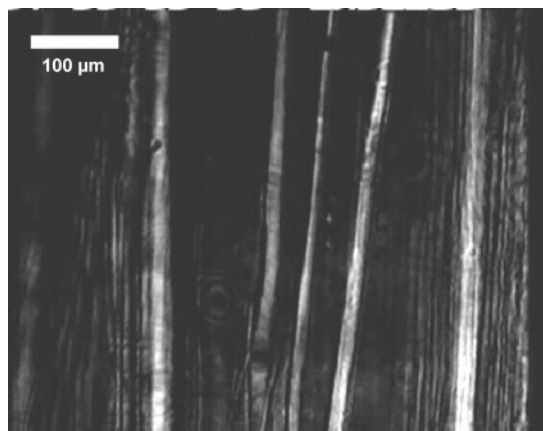


**Figure 2.** Fracture texture of a collapsed DPPC/DPPS monolayer for $x = 0.20$ and $\pi_c = 62$ mN/m as observed with Brewster angle microscopy. Folds travel perpendicular to the horizontal compression direction. The length of the folds is larger than the separation between the folds, which in turn is larger than the width of the folds.

mersed into the aqueous solution before lipids were spread on the air/water interface and was drawn out smoothly after the monolayer collapsed.

**Results**

**Isotherms.** The pressure−area isotherms of pure DPPS and DPPS/DPPC mixtures are shown in Figure 1. Constant-speed compression decreases the available area of each molecule, and the monolayer pressure increases until the molecular area reaches a limiting value above which the monolayer is closest packed and cannot be compressed further. $\pi_C$ is defined as such a critical (collapse) surface pressure, and above this limiting condition the packed monolayer will collapse. We denote the molar fraction of DPPC as $x = [\text{DPPC}]/([\text{DPPS}] + [\text{DPPC}])$. Isotherms are displayed for $x = 0$, 0.2, and 0.75. At low mole fractions of DPPC, we find a collapse pressure of roughly $\pi_C \approx 60$ mN/m. At a higher mole fraction $x$ of DPPC, the collapse pressure rises to $\pi_C \approx 70$ mN/m, which is almost the surface tension of water.

**Collapse Textures.** Anisotropic collapse upon uniaxial compression is observed for $x < 0.25$. Figure 2 shows a typical collapse pattern of a monolayer with $x = 0.2$. Irreversible folds consisting of 3D assembly of surfactant material, visualized as bright lines using Brewster angle microscopy, span the image perpendicular to the compression direction. The length of the folds exceeds the size of the image. The separation of individual
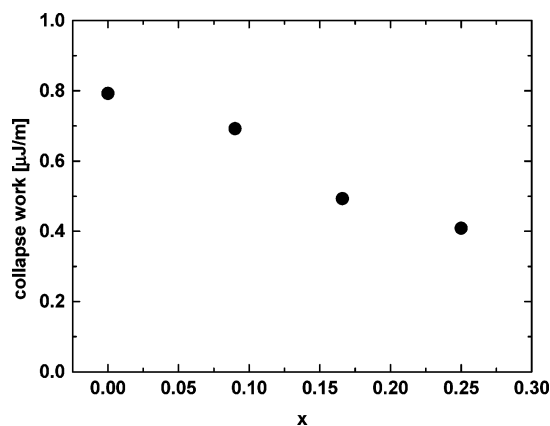


**Figure 3.** Collapse work per unit length of the crack as a function of the composition $x$.

folds is smaller than their length, and the width of the folds is smaller than their separation. In contrast to the reversible folds observed by Lipp et al.[8] and Lu et al.,[5] the folds observed here are irreversible, and the fold cannot be erased by expansion of the monolayer. Upon formation of a fold, material in a region of width of $d$ around the forming fold is transferred from the monolayer into the fold. An estimate of the collapse work performed is then simply given by $W = \pi_c d$. We measured $d$ by measuring the distance between two folds prior to and after the incorporation of an additional fold between the other two. The resulting collapse work of the folds per unit length of the fold is depicted as a function of the mole fraction $x$ of DPPC in Figure 3. As one can see the work of collapse drops by about a factor of 2 when moving from pure DPPS ($x = 0$) toward a mole fraction of DPPC of $x = 0.25$. Obviously, the addition of DPPC to the monolayer softens the material, and the collapse work therefore decreases.

We found that the kinetics of fold formation depends on the time lag between the spreading and compression of the film on the air/water surface. If the compression follows directly after spreading the monolayer, a straightforward propagation of the fold edge is observed. However, if we leave the monolayer for equilibration for an hour before we compress the monolayer, the propagation speed of the fold edge is much faster and cannot be resolved by the fast CCD camara. Consecutive secondary folds that travel within the primary fold and enlarge and intensify the primary fold, however, are slower. The kinetics of these secondary folds, therefore, can be resolved with our camera system.

The evolution of a single primary fold, where the compression directly follows the spreading is depicted in Figure 4 for $x = 0.09$ Figure 4a depicts a virgin monolayer. Four milliseconds later, a primary fold appears approximately perpendicular to the compression direction. It propels forward through the monolayer with a speed of 36 mm/s. The last image in Figure 4 shows a similar fold an hour after formation of the fold and after expansion to negligible surface pressure. Clearly, the fold formation is irreversible, and no reformation of a monolayer is observed.

In a monolayer equilibrated for an hour after the phospholipids were spread, primary folds propagate much faster. Figure 5 shows the fold formation in such an equilibrated monolayer. The first image ($t = 0$) shows the monolayer right before the collapse. In the second image $t = 4$ ms later, a modulated fold has propelled through the entire image and the primary fold speed is too fast to be measured. However, the fold growth is followed by secondary folds after roughly 100 ms which travel
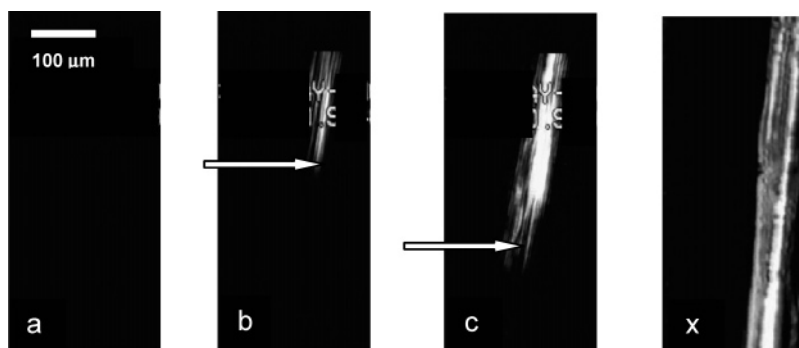
**Figure 4.** Growth of a primary fold of a mixed DPPC/DPPS monolayer with $x = 0.09$ compressed at a rate of $-0.1$ Å$^2$/mol·s. Parts a–c are consecutive images separated by a time lag of 4 ms. Fig x shows the fold after expansion to zero surface pressure and after a waiting time of 1 h.
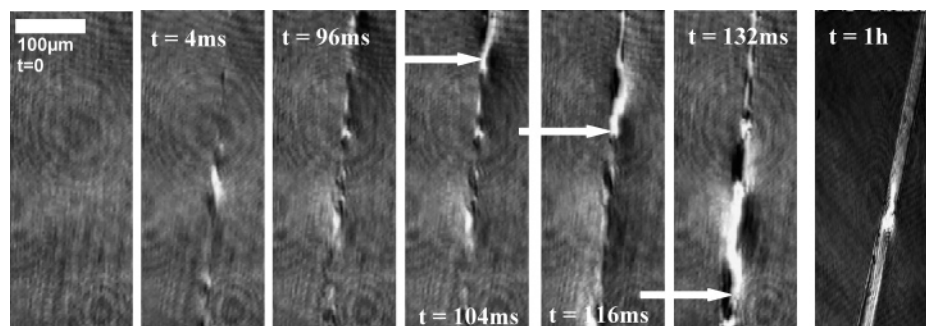


**Figure 5.** Fracture kinetics in a pure DPPS monolayer compressed at a rate of $-0.1$ Å$^2$/mol·s. A primary fold is formed within 4 ms. A secondary fold travels through the primary fold between $t = 96$ and $132$ ms (white arrows). The last image shows the fold after a settling time of 1 h.
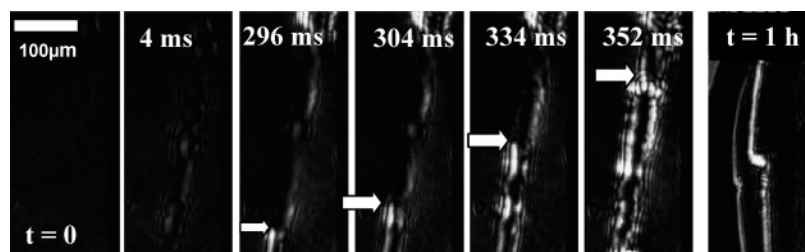


**Figure 6.** Fold growth of a DPPC/[DPPS + DPPC] monolayer with $x = 0.25$ compressed at a rate of $-0.1$ Å$^2$/mol·s. A primary fold is formed within 4 ms. A secondary fold travels through the primary fold between $t = 296$ and $352$ ms (white arrows). The last image shows the fold after a settling time of 1 h.

through the primary fold and thereby enlarge the primary fold (arrows in Figure 5). The fold speed of those secondary folds can be resolved in time with the fast camera, and we find typical values in the range of $v = 11$ mm/s. When expanding the monolayer to zero surface pressure, the primary and secondary folds persist. The last image in Figure 5 shows a fold after a 1-h waiting time. Again, the fold is an irreversible structure.

The fold dynamics of DPPC–DPPS mixtures can be changed by varying the mole fraction $x$ of DPPC. For $x < 0.2$, the collapse morphologies of mixtures are similar to those of the pure DPPS. The more DPPC added, the slower the propagation speed of secondary folds. Figure 6 shows the formation of a primary fold and subsequent secondary fold forming in a monolayer with $x = 0.25$.[16] Here, the average secondary fold edge speed is around $v = 5.2$ mm/s, almost half of the value for pure DPPS. The width of the primary fold enlarges after the passage of the secondary fold. The last image in Figure 6 is a typical post fold pattern observed on an expanded surface ($\pi = 0$), proving the irreversibility of the event. For $x > 0.5$, we no longer observe the formation of folds, and the collapse pressure $\pi_c \approx 71.0$ mN/m almost equals the surface tension of water. Presumably, the monolayers reversibly fold into the subphase as described for pure DPPC.[5,8] The morphology of
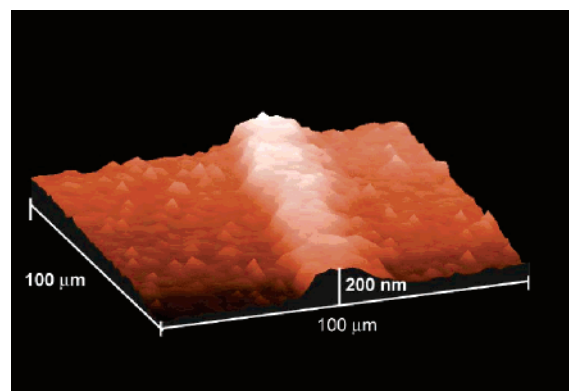


**Figure 7.** Profile of a fold on a silicon substrate of a transferred collapsed DPPC/ DPPS monolayer with $x = 0.2$ re-expanded to zero pressure prior to transfer.

the folds was recorded by transferring the film onto a silicon wafer using the Langmuir–Schäfer technique.

Figure 7 shows a profile of a fold in a monolayer with $x = 0.20$ transferred at a surface pressure of $\pi = 0$ mN/m. It is well-known that the morphology of a film can be distorted when undergoing a LB transfer. However, the agreement of the profilometer image with the BAM images on the air/water
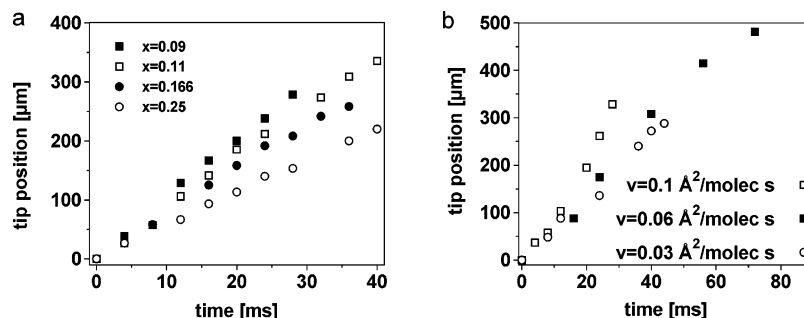
Fold Speed in Monolayers

*J. Phys. Chem. B, Vol. 109, No. 8, 2005* **3445**



**Figure 8.** Secondary fold length as a function of time for different composition $x$ and compression rates. The fold length increases linearly with time.
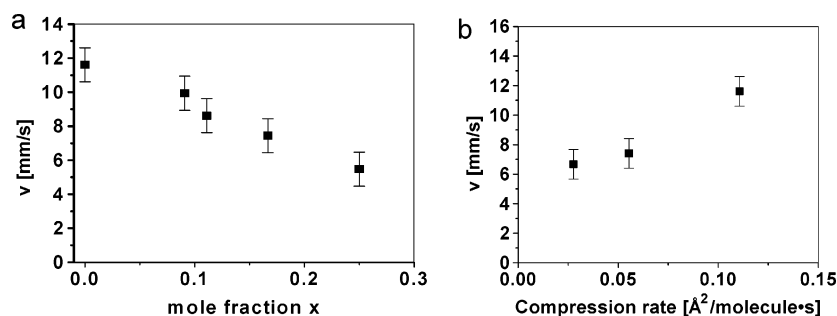


**Figure 9.** Secondary fold speed $v$ as a function of the mole fraction $x$ of DPPC and the compression rate.

surface suggests that no major rearrangement occurred during transfer. The profilometer images show folds appearing as straight ridges of typical height of 80−300 nm and width of 20 $\mu$m.

In parts a and b of Figure 8, we plot the secondary fold edge position vs time for different compositions $0 < x < 0.25$ and compression rates of the monolayers. All curves obey a simple linear relation, with secondary fold speeds that slow upon addition of DPPC. The fold speed increases with the compression rate. Figure 9 summarizes these findings in plots of the secondary fold speed as a function of $x$ and of the compression rate.

**Discussion**

Our experiments demonstrate that there are two distinct collapse evolutions for a DPPS/DPPC monolayer, depending on the composition ratio. At low $x$, anisotropic fracture creates irreversible folds, the kinetics of which depend on the waiting time between spreading and compression. At high $x$, the monolayer reversibly folds into the subphase. The low $x$ fold growth is uniaxial with folds traveling perpendicular to the compression. Brener et al.[11] developed a theory for uniaxially stressed 3D solids. Interestingly, they predict the formation of cracks that grow in length linearly with time, leading to a coarsening of the crack structure predicted to consist of parallel cracks separated by distances that are small compared to the length of the cracks. In our system, which fulfills the hierarchy of length scales required by the theory, we observe such linear growth of folds. Obviously our system is 2D rather than 3D, with a reversed sign of the stress as compared to the system studied by Brener et al., but we believe that this basic prediction should not be altered as we change the dimension of space. A theoretical description of fold formation similar to Brener et al.[11] adapted to 2D systems could help a better understanding of fold formation in 2D monolayers.

**Conclusion**

The collapse of mixed DPPS/DPPC monolayers at low mole fraction of DPPC occurs by the formation of anisotropic

irreversible folds. Fast primary folds are followed by secondary folds that travel at a constant speed. The collapse work and the secondary fold speed decreases with increasing $x$. The secondary fold formation bares similarities with theoretical predictions for the crack coarsening dynamics of uniaxially stressed 3D solids.[11]

**References and Notes**

(1) Adamson, A. W.; Gast, A. P. *The Physical Chemistry of Surfaces*, 6th ed.; John Wiley & Sons: 1997.

(2) Angelova, A.; Vollhardt, D.; Ionov, R. *J. Phys. Chem.* **1996**, *100*, 10710.

(3) Schief, W. R.; Touryan, L.; Hall, S. B.; Vogel, V. *J. Phys. Chem. B* **2000**, *104*, 7388.

(4) Schief, W. R.; Hall, S. B.; Vogel, V. *Phys. Rev. E* **2000**, *62*, 6831.

(5) Lu, W. X.; Knobler, C. M.; Bruinsma, R. F.; Twardos, M.; Dennin, M. *Phys. Rev. Lett.* **2002**, *89*, 146107. Ybert, C.; Lu, W. X.; Möller, G.; Knobler, C. M. *J. Phys. Chem. B* **2002**, *106*, 2004.

(6) Hatta, E.; Suzuki, D.; Nagao, J. *Eur. Phy. J.* **1999**, *B11*, 609.

(7) Hatta, E.; Fischer, T. M. *J. Phys. Chem.* **2002**, *106*, 589.

(8) Lipp, M. M.; Lee, K. Y. C.; Takamoto, D. Y.; Zasadzinski, J. A.; Waring, A. J. *Phys. Rev. Lett.* **1998**, *81*, 1650. Diamant, H.; Witten, T. A.; Gopal, A.; Lee, K. Y. C. *Europhys. Letter.* **2000**, *52*, 171. Gopal, A.; Lee, K. Y. C. *J. Phys. Chem. B* **2001**, *105*, 10348.

(9) Ries, H. E., Jr. *Nature* **1979**, *281*, 287.

(10) Griffith, A. A. *Philos. Trans. R. Soc. London, Ser. A* **1920**, *221*, 163.

(11) Brener, E. A.; Müller-Krumbhaar, H.; Spatschek, R. *Phys. Rev. Lett.* **2001**, *86*, 1291.

(12) Holian, B. L.; Blumenfeld, R.; Gumbsch, P. *Phys. Rev. Lett.* **1997**, *78*, 78.

(13) Sharon, E.; Gross, S. P.; Fineberg, J. *Phys. Rev. Lett.* **1995**, *74*, 5096. Sharon, E.; Cohen, G.; Fineberg, J. *Phys. Rev. Lett.* **2002**, *88*, 085503.

(14) Blumenfeld, R. *Phys. Rev. Lett.* **1996**, *76*, 3703.

(15) Ching, E. S.; Langer, J. S.; Nakanishi, H. *Phys. Rev. Lett.* **1996**, *76*, 1087.

(16) Primary folds occur at random positions. The primary fold in Figure 5 occurs ~150 $\mu$m from where the focal plane of the BAM objective intersects with the monolayer. In contrast to Figure 4, the fold is blurred and the secondary fold seems to be somewhat displaced from the primary fold. This, however, is an artifact arising from both primary and secondary fold not being in focus.